Heat induced nanoforms of Zinc oxide quantum dots and their characterization

© Anindita Dey, Ruma Basu*, Sukhen Das¶, Papiya Nandy

Physics Department, Jadavpur University,
700032 Kolkata, India
* Physics department, Jogamaya Devi College,
700026 Kolkata, India

(Получена 21 марта 2011 г. Принята к печати 28 июня 2011 г.)

In our studies we observed heat induced phase transitions of Zinc oxide quantum dots at 60, 200, 360 and 400°C, where all the transitions were irreversible except the transition at 60°C which was a reversible one. The phase transition at 60°C indicated a heat induced conformational change which was supported here by studying polarizing micrographs of ZnO quantum dots thin film. The X-ray diffraction studies of the sample fired at different temperatures as indicated by the thermal analysis were performed in order to understand the changes occurred due to transitions. The study also indicated a new and simple approach to develop ZnO nanorods by just thermal decomposition of the ZnO quantum dots firing in furnace at 200°C with 2 h soaking. In order to have a proper insight of the structural changes we performed scanning electron microscopy. Optical characterization was done by UV-vis and fluorescence spectrophotometer.

1. Introduction

ZnO as a metal oxide semiconductor having a band gap of 3.37 eV and has a large exciton binding energy of 60 meV [1]. Owing to some special properties of ZnO nanoparticle such as larger specific surface, sensitivity to the surrounding perturbants, high surface activity etc [2] and has recently been successfully used in laser diode [3], optical wave guides [4,5], optical switches [6,7], transparent ultra violate (UV) protection conducting film [8], solar cells [9,10], gas sensing devises [11], DNA sequence sensors [12], bioimaging [13] and others. The quantum dots (QDs) are immensely applicable in different fields owing to their larger surface area and lower volume density of point defects [14]. ZnO nanorods (NRs) can be used in solar cells [15,16], photocatalytic devises [17], spin polarized light sources [18], gas and chemical sensor [19] etc.

In our experiment we have studied the heat induced changes of ZnO in its nanoform by differential thermal and thermo gravimetric analysis (DTA–TGA), and observed phase transitions at different temperatures. In order to get further information about the structural changes we have performed absorption and fluoerscence spectroscopy, X-ray diffraction studies, transmission and scanning electron microscopy.

Our result indicated that ZnO went through distinct phase transitions when fired in furnace within a specified temperature range. This is a simple and low cost method for getting the ZnO NRs from ZnO QDs form.

2. Methods

2.1. Sample materials

For sample preparation we used zinc acetate dihydrate $[Zn(Ac)_2, 2H_2O]$ from Merck, India, lithium hydroxide monohydrate $[LiOH, H_2O]$ from Loba Chemie, India and absolute ethanol (Merck, Germany) without further purification.

2.2. Sample preparation

ZnO QDs were prepared according to the procedure described by Spanhel and Anderson [20], with some modifications in the initial stage where, instead of refluxing the ethanolic zinc acetate solution for 3 h, we stirred it for 30 min at 60°C. The above prepared ZnO QDs (sample A) was fired in furnace separately at 200 (sample B), 360 (sample C) and 400°C (sample D) with 2 h shocking and all the above prepared samples were there after used for further characterization.

2.3. Investigation methods

The ZnO QDs and its heat induced different forms were characterized by using the following techniques. X-ray diffraction (XRD) spectra were recorded on Bruker AXS type diffractometer using CuK_α radiation — 1.5409 Å ($2\theta = 10-70°$, scan speed — 0.2 s/step, increment — 0.02). Thermal analysis was performed by using DTA–TGA (DTG–60 H, Shimadzu) and the images of different phases under cross polarizer were taken by using a polarizing microscope (Leitz Wetzlar Germany; Type 307-107.002514636; Max. 100 W). Absorption spectroscopy was performed in a Perkin Elmer Lambda 25 UV-vis. Sperctrometer (Shelton, CT064844794) whereas fluorescence spectral data were recorded by using Perkin Elmer luminescence spectroscopy (LS 50 W). Particle size and surface morphology of the sample were observed using high resolution transmission electron microscope (HRTEM, JEM 2010 JEOL Ltd., Tokyo, Japan) and field emission scanning electron microscopy (FESEM, JSM 6700F, JEOL Ltd., Tokyo, Japan) respectively.

¶ E-mail: sukhendasju@gmail.com

3. Result and discussion

3.1. DTA–TGA analysis

Analysis of the DTA–TGA curve of sample A within the temperature range 27 to 400°C was performed and the associated phase transitions and corresponding enthalpy required for the changes were also calculated. The simultaneous DTA–TGA showed two endothermic peaks near 60°C and 160°C and one exothermic peak at 350°C (Fig. 1, *a*). Moreover the DTA curves of sample A within temperature range 27 to 200°C (Fig. 1, *b*) showed that the first endothermic peak at about 60°C was reversible indicating the transition of ZnO QDs whereas the second endothermic and third exothermic peaks were not reversible. These two peaks appeared due to thermal lattice vibration; especially the third exothermic peak was responsible for a compact well crystal structure formation of ZnO as also being supported by the XRD pattern. The changes in enthalpy associated with these transformations were calculated from thermal analysis (Table 1). It was evident from the TGA curve that there was no weight loss during reversible transition which also supported our proposition of structural change at 60°C.

3.2. X-ray diffraction analysis

XRD spectra clearly indicated that sample A was in quantum dot form whose particle size ranges between 7–10 nm (Fig. 2, spectrum *1*). The XRD spectrum of sample B (Fig. 2, spectrum *2*) had shown more intense diffraction peaks than sample A indicating the transformation of ZnO QDs into the NRs form [2]. It was evident from the XRD spectra of sample C and D that the structure became well defined crystalline one (Fig. 2, spectra *3* and *4*) as all the diffraction peaks became sharpen. Naturally ZnO in its

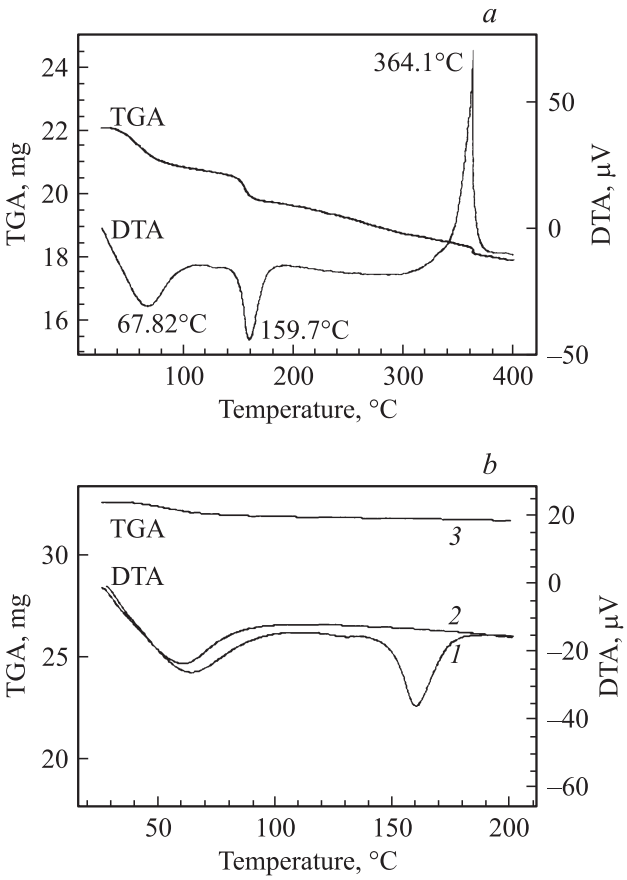

Figure 1. The differential thermal analysis (DTA) and thermogravimetric analysis (TGA) curves for ZnO quantum dots at different temperatures, °C: *a* — upto 400, *b* — upto 200. DTA and TGA curves are marked in the figures. In Fig. 1, *b*: DTA curve *2* — after cooling the sample and reheating upto 200°C showing the reversibility of the first endothermic peak.

Table 1. Details of enthalpy changes of ZnO quantum dots

Serial number	Type of reaction	Reaction range			Enthalpy (J/g)
		Start	Peak	End	
1	Endothermic	26.79	67.8	111.82	−197.03
2	Endothermic	131.67	159.7	189.26	−117.96
3	Exothermic	289.86	364.1	389.49	291.92

Table 2. Particle size of different samples calculated from XRD data

Sample	Particle size, nm [Approximation]
Sample A	5–8
Sample B	100
Sample C	150
Sample C	150
Sample D	162

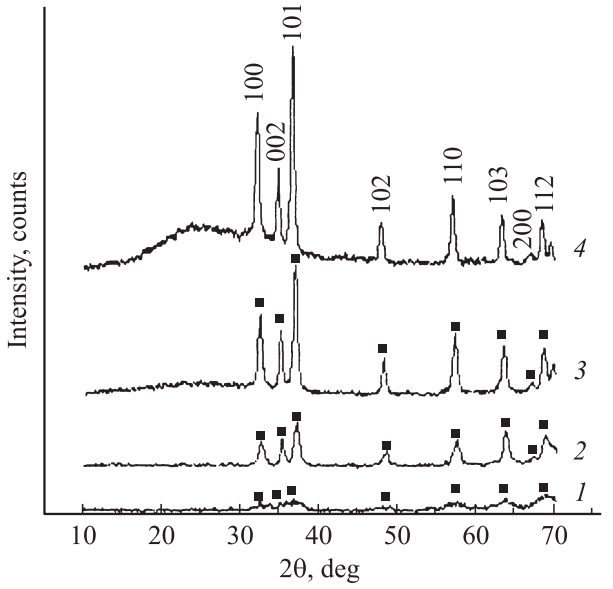

Figure 2. X-ray diffraction patterns of different ZnO nanoforms: *1* — sample A, *2* — sample B, *3* — sample C and *4* — sample D.

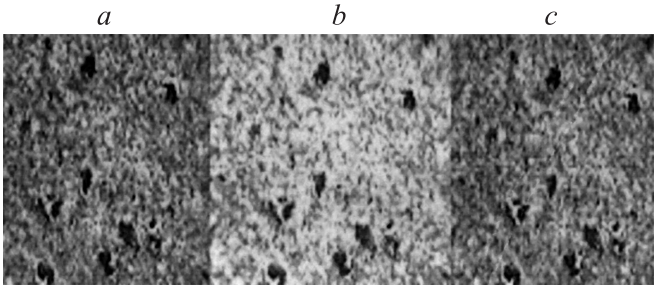

Figure 3. Polarising micrograph images of ZnO QDs: *a* — heating to 40°C, *b* — heating to 60°C and *c* — cooling to 40°C.

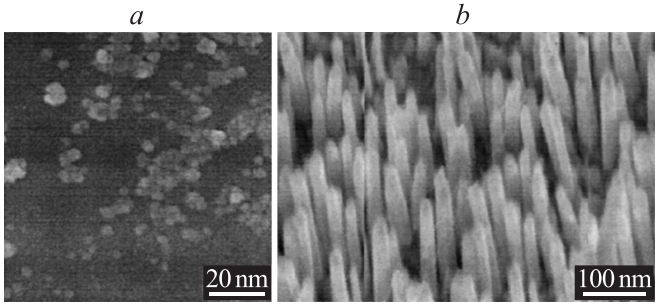

Figure 4. *a* — HRTEM image of ZnO QDs (×85.000 times), *b* — FESEM image of as prepated ZnO nanorod.

nanoform remains the stay in most stabilized wurtzite form and our X-ray diffraction spectra (Fig. 3, *a, b, c*) also match closely with those of bulk wurtzite [21]. The grain sizes of ZnO QDs as shown in Table 2, were obtained by fitting the XRD data to the Debye Scherrer formula [22] and the average crystalline size was calculated from the full-width at half-maximum (FWHM) of the XRD lines.

3.3. Electron microscopic analysis

HRTEM image of sample A was shown in Fig. 4, *a*. Although agglomeration was present to some extent, QDs indicated its particle size from 7 to 10 nm. Fig. 4, *b* showed the FESEM image of ZnO NRs. Average length and width of ZnO NRs were 100–150 nm and 25–40 nm respectively.

3.4. Polarizing micrographs analysis

Sample A was sonicated in distilled water for few minutes and a thin film was prepared with this dispersed solution. Polarizing micrographs of QDs thin film were obtained under different temperatures. When heated at 40°C the picture (Fig. 4, *a*) became hazy whereas at 60°C it was quite sharp (Fig. 4, *b*) i. e. a phase transition as indicated by the change in birefringence of the sample was observed which came back to the previous one when the temperature was lowered to 40°C (Fig. 4, *a*). This result also indicated a heat induced conformational change of ZnO QDs at a specific temperature (near about 60°C) which was also clearly observed in our DTA study.

4. Spectral data analysis

4.1. UV–visible spectroscopy

Absorption spectra of ZnO in different nanoforms were taken using colloidal suspension of the samples. Dispersion of all the samples in distilled water was conducted in an ultrasonic bath (Imico Ultrasonic, India) for 20 min. Absorption spectra of sample A and all three fired samples were illustrated in Fig. 5. It was seen that sample A showed a marked absorption in the broad range of 350–370 nm (Fig. 5, graph *1*). It was noticed that the absorption peaks gradually became more prominent in the fired samples. In case of sample B absorption maximum was at 361 nm (Fig. 5, graph *2*) where as at 369 and 372 nm approximately in case of sample C (Fig. 5, graph *3*) and sample D (Fig. 5, graph *4*) respectively. Not only the absorption peaks became prominent but also a clear gradual red shift was noticed in all the fired samples which also indicated that agglomeration took place in all the fired samples. So, the spectral data fully obeyed the size quantization effect that explained a gradual blue shift of absorption band with the decrease of particle size [23].

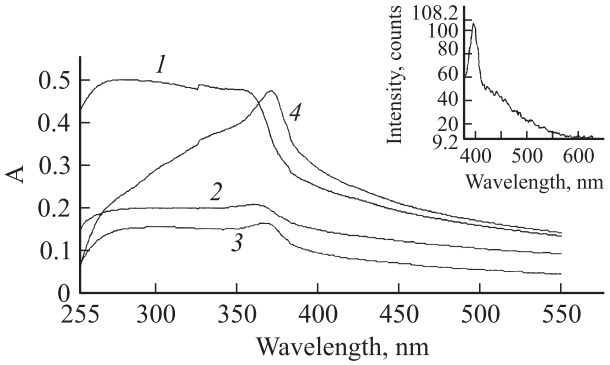

Figure 5. UV-visible absorption spectra of sample A (graph *1*), sample B (graph *2*), sample C (graph *3*) and sample D (graph *4*). Fluorescence spectrum of 398 nm emission of ZnO QD in the inset.

4.2. Fluorescence spectroscopy

ZnO in its nanoforms show various luminescence transitions depending on different preparation techniques leading to structural and surface properties variation. ZnO nanocrystals prepared in aqueous solution generally exhibit a broad visible luminescence centered at 530 nm and a UV emission band attributed to exciton recombination [24]. However in our studies the fluorescence spectrum of sample A for an excitation wavelength of 360 nm showed maximum emission peak at 398 nm (Fig. 5, inset) and a gradual red

shift was noticed in case of sample B, C and D (maximum emission peaks at 411, 422 and 425 nm respectively). Moreover a prominent shoulder in the green region was also observed in all the cases.

The photoluminescence of ZnO QDs in aqueous suspension suggests that UV luminescence is due to the transition from conduction band edge to valence band, and the luminescence in visible range is caused by the transition from deep donor level to valence band due to oxygen vacancies and by the transition from conduction band to deep acceptor level due to impurities and defect states [25].

In all of our four samples the intensity of the green light emission was relatively weak owing to low oxygen vacancies as we know that green light emission commonly referred to as a deep-level or trap-state emission [26] is caused by the radiative recombination of a photogenerated hole with an electron occupying the singly ionized oxygen vacancy in ZnO [27].

5. Conclusion

From all the experimental data two main things can be concluded. Firstly, from the thermal data analysis it was shown that one of the two endothermal peaks in DTA was reversible. The reversible phase transition that leads to heat induced conformational change as shown in polarizing micrograph images was a unique feature of our study. This conformational change may have immense importance in other fields. Further studies about this are in progress. Secondly X-ray analysis proved the conversion of ZnO QDs to NRs by application of heat only (at 200°C) as well as the well crystalline nature of QDs at higher temperature (at 360 and 400°C). As these conformational changes of ZnO QDs can obtain by application of heat only, instead of chemical treatment, this is a major breakthrough as both QDs as well as NRs have ample applications in different fields. The process adopted in our experiments was time as well as energy saving one.

Acknowledgement: we gratefully acknowledge the Department of Science & Technology, Government of West Bengal, for financial support in our research work.

References

[1] U. Ozgur, Y.I. Alivov, C. Liu, A. Teke, M.A. Reshchikov, S. Dogan, V. Avrutin, S.J. Cho, H.J. Morkoc. J. Appl. Phys., **98**, 041 301 (2005).
[2] Y. Lin, D. Wang, Q. Zhao, M. Yang, Q. Zhang. J. Phys. Chem. B, **108**, 3202 (2004).
[3] R.F. Service. Science, **276**, 895 (1997).
[4] K.H. Guenther. Appl. Optics, **23**, 3612 (1984).
[5] F.C.M. Van De Pol. Ceramic Bulletin, **69**, 1959 (1990).
[6] K. Nashimoto, S. Nakamura, H. Mariyama. Jpn. J. Appl. Phys., **43**, 5091 (1995).
[7] T. Nagata, T. Shimura, A. Asida, N. Fujimura, T.J. Ito. Cryst. Growth, **237**, 537 (2002).
[8] Y.J. Lin, Y.W. Kwon, Y.W. Heo, J. Zhou, S. Luo, P.H. Holloway, E. Douglas, D.P. Norton, Z. Park, S. Li. Semicond. Sci. Technol., **20** (8), 720 (2005).
[9] Z. Guo, S. Wei, B. Shedd, R. Scaffaro, T. Pereira, H. Thomas. J. Mater. Chem., **17**, 806 (2007).
[10] E. Hosono, S. Fujihura, I. Honma, H.H. Zhou. Adv. Mater., **17**, 2091 (2005).
[11] M. Yang, D. Wang, L. Peng, T. Xie, Y. Zhao. Nanotechnology, **17**, 4567 (2006).
[12] N. Kumar, A. Dofiman, J. Hahm. Nanotechnology, **17**, 2878 (2006).
[13] H.M. Xiong, Y. Xu, Q.G. Ren, Y.Y. Xia. J. Am. Chem. Soc., **130**, 7522 (2008).
[14] *Nanomaterials: Synthesis, Properties and Applications*, eds by A.S. Edelstein, R.C. Cammarata. (Institute of Physics Publishing, Bristol, 1996).
[15] K.S. Kim, Y.S. Kang, J.H. Lee, Y.J. Shin, N.G. Park, K.S. Ryu, S.H. Chang. Bull. Corean Chem. Soc., **26** (12), 1921 (2005).
[16] D. Wei, H.E. Unalan, D. Han, Q. Zhang, L. Niu, G. Amaratunga, T.A. Ryhanen. Nanotechnology, **19**, 424 006 (2008).
[17] I. Poulios, D. Makri, X. Prohasha. Global Nest Int. J., **1**, 55 (1999).
[18] D.P. Norton, S.J. Pearton, A.F. Hebard. Appl. Phys. Lett., **88**, 239 (2003).
[19] H. Wang, B.S. Kang, F. Ren. Appl. Phys. Lett., **87**, 172 105 (2005).
[20] L. Spanhel, M.A. Anderson. J. Am. Chem. Soc., **113**, 2826 (1991).
[21] L.P. Snedeker, A.S. Risbud, O. Masala, J.P. Zhang, R. Seshadri. Sol. St. Sci., **7**, 1500 (2005).
[22] I.E. Alexander, H.P. Klug. *X-ray diffraction procedures for polycrystaline and amorphous materials* (N.Y., Wiley and Sons, 1954) Chap. 7.
[23] A.B. Djuristic, Y.H. Leung. Mater. View. Com., **2**, 944 (2006).
[24] D.S. Bohle, C.J. Spina. J. Am. Chem. Soc., **129**, 12 380 (2007).
[25] L. Irimpan, V.P.N. Nampoori, P. Radhakrisnan, A. Deepthy, B. Krishnan. J. Appl. Phys., **102**, 063 524 (2007).
[26] R. Viswanatha, S. Sammer, B. Satpati, P.V. Satyam, B.N. Dev, D.D. Sharma. J. Mater. Chem., **14**, 661 (2004).
[27] K. Vanheusden, W.L. Warren, C.H. Seager, D.R. Tallant, J.A. Voigt. J. Appl. Phys., **79**, 7983 (1996).

Редактор Т.А. Полянская